Preparation of Nanomaterials

Dr. Pallab Ghosh
Associate Professor
Department of Chemical Engineering
IIT Guwahati, Guwahati–781039
India

Table of Contents

9.2.1 Preparation of nanoparticles

- Metal nanoparticles are used as various types of catalysts, adsorbents, sensors and ferrofluids. They have applications in optical, electronic and magnetic devices. Most of these applications critically depend on the size and shape of the nanoparticles. Therefore, the synthesis of well-controlled size and shape of these nanoparticles is important for these applications.
- The reduction of metal complexes to form metallic colloid dispersions is a very common technique. Various precursors, reducing agents and polymeric stabilizers are used in the preparation of metallic colloid dispersions. Some of these are presented in Table 9.2.1.

Table 9.2.1 Precursors, reducing agents and polymeric stabilizers used in the preparation of metallic nanoparticles

Category	Name
Precursor	Metal anode
	Palladium chloride
	Potassium tetrachloroplatinate II
	Silver nitrate
	Chloroauric acid
	Rhodium chloride
Reducing agent	Hydrogen
	Sodium citrate
	Citric acid
	Carbon monoxide
	Methanol
	Formaldehyde
	Hydrogen peroxide
	Sodium tetrahydroborate
Polymeric stabilizer	Poly(vinylpyrrolidone)
	Polyvinyl alcohol

	Sodium polyphosphate
	Sodium polyacrylate

- The size of metallic colloids varies significantly with the type of the reducing agent. A strong reducing agent promotes a fast reduction reaction, and if the reaction is fast, generally small nanoparticles are formed. On the other hand, a weak reducing agent induces a slow reaction and usually large particles are formed.
- A strong reducing agent generates an abrupt surge of the concentration of the growth species resulting in a very high supersaturation. Consequently, a very large number of nuclei are formed initially. For a given concentration of the metal precursor, the formation of a large number of nuclei results in small size of the nanoparticles.
- The role of polymeric stabilizer is to form a monolayer on the surface of the nanoparticles and prevent their aggregation. The polymeric stabilizer is also known as a *capping material*. The monolayer of the polymer, however, can affect the growth process significantly. If the growth sites are occupied by the polymer, the rate of growth of nanoparticles may be reduced. If the polymeric stabilizer completely covers the surface of the growing particle, it may hinder the diffusion of the growth species from the surrounding solution to the surface of the particle.
- The shape of the nanoparticles can be varied by the use of different amounts of the polymeric stabilizer. The shape and size of platinum nanoparticles have been controlled by changing the ratio of the concentration of the polymer (sodium polyacrylate) to the concentration of the platinum cations (Ahmadi *et al*., 1996). They observed tetrahedral, cubic, irregular-prismatic, icosahedral and cubo-octahedral shapes of the particles, as shown in Fig. 9.2.1.
- Gold nanoparticles are well known for their distinct colors (see Lecture 3 of Module 1). They have been used in glasses and enamels as coloring agents (see Fig. 9.2.2). A variety of methods exist for the preparation of gold nanoparticles. One of the most common methods is the reduction of chloroauric acid at 373 K by sodium citrate.

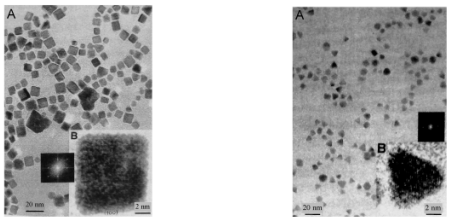

(a) (b)

Fig. 9.2.1 TEM images of platinum nanoparticles: (a) cubic nanoparticles formed when the initial ratio of concentration of polymer (sodium polyacrylate) to that of the metal cation in the solution was 1:1, and (b) tetrahedral nanoparticles formed when the initial ratio was 5:1. The insets show high-resolution images of the particles (Ahmadi *et al*., 1996) (reproduced by permission from The American Association for the Advancement of Science, © 1996).

Fig. 9.2.2 Glass carafe in which gold nanoparticles are dispersed (this glass is known as *ruby glass*).

- To prepare a colloidal dispersion of rhodium, the following reduction reaction, using methanol as the reducing agent, can be carried out in presence of a stabilizer such as polyvinyl alcohol.

$$2RhCl_3 + 3CH_3OH \rightarrow 2Rh + 3HCHO + 6HCl \qquad (9.2.1)$$

- The size of nanoparticles depends on the reaction conditions. Ostwald ripening plays an important role in the size of the nanoparticles. Nanoparticles of platinum and palladium can be prepared by reduction using hydrogen: the salts K_2PtCl_4 and $PdCl_2$ are hydrolyzed to form hydroxides, which are then reduced.

$$PdCl_2 + Na_2CO_3 + 2H_2O \rightarrow Pd(OH)_2 + H_2CO_3 + 2NaCl \qquad (9.2.2)$$

$$Pd(OH)_2 + H_2 \rightarrow Pd + 2H_2O \qquad (9.2.3)$$

- Non-oxide semiconductor nanoparticles can be synthesized by the pyrolysis of organometallic precursor dissolved in anhydrate solvents at elevated temperatures in airless environment in presence of a polymeric stabilizer. The nanocrystals of CdS, CdSe and CdTe have been prepared in this method. The nanocrystals of GaN have been synthesized by a thermal reaction of Li_3N and $GaCl_3$ at 553 K under pressure using benzene as the solvent in argon atmosphere (Xie *et al*., 1996).

$$GaCl_3 + Li_3N \rightarrow GaN + 3LiCl \tag{9.2.4}$$

- The yield of GaN was 80% and the size of the particles was 30 nm. The product comprised of mostly hexagonal GaN with a small amount of rocksalt GaN.
- A well known method for synthesizing oxide nanoparticles is sol–gel processing. The sol–gel process typically consists of hydrolysis and condensation of the precursors. The typical precursors are metal alkoxides, or inorganic and organic salts. The precursors are dissolved in aqueous or organic solvents. Sometimes catalysts are used to promote the hydrolysis and condensation reactions.

$$GaCl_3 + Li_3N \rightarrow GaN + 3LiCl \tag{9.2.5}$$

$$\text{Hydrolysis: } M(OEt)_4 + xH_2O \Leftrightarrow M(OEt)_{4-x}(OH)_x + x\text{EtOH} \tag{9.2.6}$$

Condensation: (9.2.7)

$$2M(OEt)_{4-x}(OH)_x \Leftrightarrow (OEt)_{4-x}(OH)_{x-1}MOM(OEt)_{4-x}(OH)_{x-1} + H_2O$$

where M represents the metal. The nanoclusters formed by condensation often have organic groups attached to them, which may result due to incomplete hydrolysis.

- The size of the nanoclusters and the structure of the final product can be tailored by suitably controlling the reactions. Colloidal dispersions of metal hydrous oxides consisting of particles of considerable uniformity in size and shape have been synthesized by keeping the salt solutions of the respective metals at elevated temperatures for various periods of time.
- The particle shape and composition depend most strongly on the pH and on the nature of the anions contained in the aging systems. Ferric oxide nanoparticles were synthesized by aging ferric salt solutions with the corresponding acid at 373

K for one day. Electron micrographs of ferric oxide nanoparticles formed from $Fe(NO_3)_3$ & HNO_3, and $Fe(ClO_4)_3$ & $HClO_4$ solutions are shown in Fig. 9.2.3.

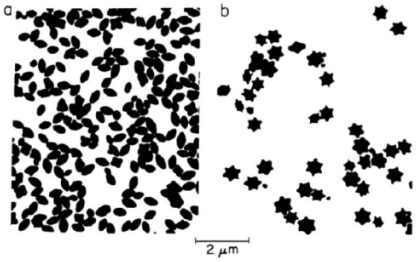

Fig. 9.2.3 Electron micrographs of iron oxide nanoparticles obtained by aging the solutions at 373 K for one day: (a) $Fe(NO_3)_3$ (18 mol/m^3) + HNO_3 (104 mol/m^3), and (b) $Fe(ClO_4)_3$ (18 mol/m^3) + $HClO_4$ (104 mol/m^3) (Matijević, 1977) (reproduced by permission from Elsevier Ltd., © 1977).

The anions influence the surface properties and interfacial energy of the nanoparticles, and hence the growth of the nanoparticles. They can also influence the electrostatic double layer repulsion between the particles and hence their stability.

9.2.1.1 Microemulsion-based methods

- Ultrafine metal nanoparticles of diameter between 5 nm and 50 nm can be prepared by water-in-oil microemulsions (the details of microemulsions are given in Lecture 4 of Module 6). The nanodroplets of water are dispersed in the oil phase. The size of the droplets can be varied in the range of 5–50 nm by changing the water/surfactant ratio. The surfactant molecules provide the sites for particle nucleation and stabilize the growing particles. Therefore, the microemulsion acts as a microreactor.
- The reactant metal salts and reducing agents are mostly soluble in water. Therefore, the nucleation of particles proceeds in the water pools of the microemulsion. One microemulsion contains the metal salt and the other microemulsion contains the reducing agent. The nanoparticles are synthesized by mixing the two microemulsions as shown in Fig. 9.2.4.

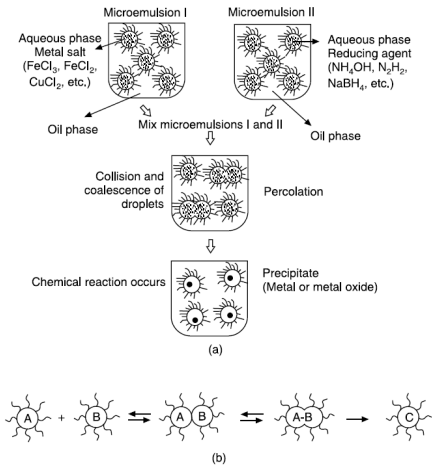

Fig. 9.2.4 (a) Mechanism for the synthesis of metal nanoparticles by the microemulsion approach, and (b) the percolation mechanism in detail (Capek, 2004) (reproduced by permission from Elsevier Ltd., © 2004).

- During the collision of the water droplets, interchange of the reactants (i.e., the metal salt and the reducing agent) takes place. The interchange of reactants is very fast so that it occurs during the mixing process itself. The nucleation and growth take place inside the droplets.
- Interchange of nuclei or particles between the drops is hindered because it would require formation of a big hole during the collision of the droplets and would require a large change in the curvature of the surfactant layer around the drops, which is not favored energetically. Since the inorganic salts have very low solubility in the oil phase, the dynamic exchange of reactants between the droplets through the continuous phase is unfavorable. When the particles attain their final size, the surfactant molecules attach themselves to the surface of the particles and stabilize them. Further growth is also prevented by the adsorbed surfactant layer.
- Percolation is a very important step in the particle nucleation. It is illustrated in the Fig. 9.2.4 (b) for a bimolecular reaction: $A + B \rightarrow C$, where A represents the metallic salt (e.g., $FeCl_3$), B represents the reducing agent (e.g., $NaBH_4$), and C represents the metal particle.
- For the reaction to occur, the reactant, A, located in the water pool of one droplet must find the reactant, B, located in the water pool of another droplet.

This can occur by two mechanisms: (i) movement of A molecule out of the water pool, migration through the oil phase and entry into the water pool containing B molecule, or (ii) direct transfer between two water pools containing molecules of A and B at the time of collision between two droplets.

- If the collisions are energetic and strongly interactive, the latter mechanism would prevail. Eicke *et al*. (1976) have shown that the inter droplet communication is very rapid and it occurs by a transitory dimer species which is formed as a result of the collision between two droplets. Generally the chemical reaction between the salt and the reducing agent is very fast compared to the communication between the droplets. Therefore, the rate determining step is the second-order communication step. The rate constant for this step is estimated to be in the range of 10^6 to 10^7 dm^3 mol^{-1} s^{-1} for Aerosol OT–water–heptane microemulsion system (Capek, 2004).
- The concentrations of the reactants affect the reduction rate. The rates of both nucleation and growth are determined mainly by the probabilities of the collisions between two atoms, between one atom and a nucleus, and between two nuclei.
- The first type of collision is related to nucleation, and the second and third types are related to the growth process. To prepare nanoparticles of different diameters, the water/surfactant ratio can be varied.
- Barnickel *et al*. (1992) have synthesized silver nanoparticles of different size by varying this ratio. The non-ionic surfactant, dodecyl-pentaethyleneglycol-ether, was used for stabilizing the reverse micelles. One w/o microemulsion solubilized $AgNO_3$, and the other microemulsion solubilized $NaBH_4$. As the water/surfactant ratio (W/S) increased from 0.05 to 0.2, the droplet size in the microemulsion increased. At the same time, the mean particle diameter increased. These results are shown in Fig. 9.2.5.

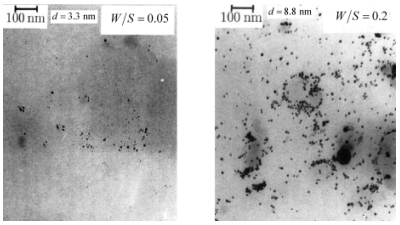

Fig. 9.2.5 Transmission electron micrographs of silver nanoparticles synthesized in w/o microemulsions. The micrographs depict the effect of water/surfactant ratio on the size of silver nanoparticles. The most probable particle diameters are indicated on the micrographs (Barnickel *et al*., 1992) (reproduced by permission from Elsevier Ltd., © 1992).

- However, with increase in water/surfactant ratio further, this trend was apparently reversed: the particle diameter decreased, although some very large particles were formed. The formation of the large aggregates was attributed to secondary growth induced by small temperature fluctuations which might have temporarily destabilized the microemulsion. The most uniform product with the narrowest size distribution was obtained for W/S = 0.2.
- Extensive literature is available on the synthesis of iron, platinum, cadmium, palladium, silver, copper, nickel and gold nanoparticles by the water-in-oil microemulsion method.

9.2.2 Carbon fullerenes

- Fullerenes are a family of carbon allotropes: molecules composed entirely of carbon in the form of a hollow sphere, ellipsoid, tube or plane. Fullerenes are similar in structure to graphite, which is composed of stacked sheets of linked hexagonal rings, but may also contain pentagonal or sometimes heptagonal rings.
- The most familiar carbon fullerene is a molecule with 60 carbon atoms, represented as C_{60}. It was discovered in 1985 by Kroto *et al*. and named as *Buckminsterfullerene*. The name was coined after the American architect Richard Buckminster Fuller who was famous for the geodesic domes built by him.

- The C_{60} molecule has a truncated icosahedral structure formed by replacing each vertex on the seams of a football by a carbon atom, as shown in Fig. 9.2.6. There are 20 hexagonal faces and 12 pentagonal faces in the molecule. The average nearest C–C distance is 0.144 nm, which is very close to that in graphite (viz. 0.142 nm). Each carbon atom is trigonally bonded to other carbon atoms, same as that in graphite.
- Out of the three bonds emanating from each carbon atom, there is one double bond and two single bonds. The hexagonal faces consist of alternating single and double bonds and the pentagonal faces are defined by single bonds. The length of the single bonds is 0.146 nm, which is longer than the average bond length (i.e., 0.144 nm), while the double bonds are shorter, viz. 0.14 nm. The diameter of the C_{60} molecule is 0.71 nm. The inner cavity is capable of holding a variety of atoms.

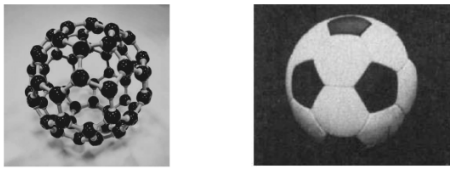

Fig. 9.2.6 The truncated-icosahedral structure of C_{60} Buckminsterfullerene (Kroto *et al*., 1985) (reproduced by permission from Macmillan Publishers Ltd., © 1985).

- This unusual molecule was synthesized by the vaporization of carbon species from the surface of a solid disk of graphite into a high-density helium flow using a focussed pulse laser. The resulting carbon clusters were expanded in a supersonic molecular beam, photoionized using an excimer laser, and detected by time-of-flight mass spectrometry. The vaporization chamber is shown in Fig. 9.2.7.
- The vaporization laser beam was focussed through the nozzle, and it struck a graphite disk which was rotated slowly. The pulsed nozzle passed high-density helium over this vaporization zone. The helium carrier gas provided the thermalizing collisions necessary to cool, react and cluster the species in the vaporized graphite plasma. Free expansion of this cluster-laden gas at the

end of the nozzle formed a supersonic beam which was probed 1.3 m downstream with a time-of-flight mass spectrometer.

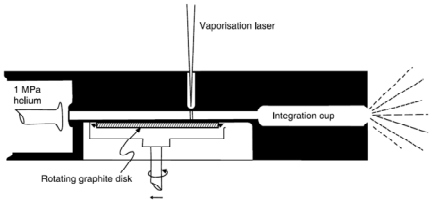

Fig. 9.2.7 Schematic of the pulsed supersonic nozzle used to generate carbon cluster beams. (Kroto *et al*., 1985) (reproduced by permission from Macmillan Publishers Ltd., © 1985).

- Other fullerenes with smaller as well as larger number of carbon atoms also exist. They are represented as C_n. Kroto (1987) has presented a set of simple, empirical chemical and geodesic rules which relate the stability of carbon cages mainly to the disposition of pentagonal rings, or various directly-fused pentagonal ring configurations. He has shown that the fullerenes with $n = 24$, 28, 32, 36, 50, 60 and 70 should have enhanced stability relative to the near neighbors.
- Fullerenes can be synthesized in large scale by the method of Krätschmer *et al*. (1990). In this method, the starting material is pure graphitic carbon soot with a few percent of C_{60} molecules. It is produced by evaporating graphite electrodes in an atmosphere of helium at about one-seventh of atmospheric pressure. The resulting black soot is scrapped from the collecting surfaces inside the evaporation chamber and dispersed in a solvent such as benzene, carbon tetrachloride or carbon disulfide.
- The C_{60} molecules dissolve to give color that varies between wine red and brown depending upon the concentration. The liquid is then separated from the soot and dried using gentle heat, leaving a crystalline residue of dark brown to black color.
- Another procedure is to heat the soot to 673 K *in vacuo* or in an inert atmosphere. The C_{60} molecules sublime out of the soot. The sublime coatings are brown to grey depending on the thickness. The details of purification methods have been given by Krätschmer *et al*. (1990).

- The low solubility of fullerenes in aqueous solution limits their applications in biology. By appropriate substitution, the fullerenes can be transformed into stabilized anions that are water soluble and can form large aggregated structures.
- A laser light scattering study of the association behavior of the potassium salt of pentaphenyl fullerene ($Ph_5C_{60}K$) in water reveals that the hydrocarbon anion, $Ph_5C_{60}^-$, associate into bilayers, forming stable spherical vesicles with an average hydrodynamic radius and a radius of gyration of ~17 nm (Fig. 9.2.8).

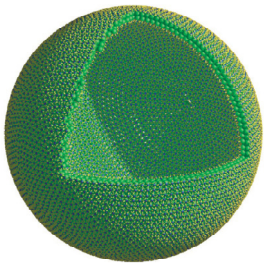

Fig. 9.2.8 A bilayer vesicle model, consisting of 6693 molecules in an outer shell (of radius 17.6 nm) plus 5973 molecules in an inner shell of radius 16.7 nm. A sector has been cut out for enhanced visibility. The hydrophobic fullerene bodies are shown in green, the hydrophilic charged cyclopentadienide regions are in blue, and the five substituents are schematically represented as yellow sticks (Zhou et al., 2001) (reproduced by permission from The American Association for the Advancement of Science, © 2001).

9.2.3 Synthesis of nanowires, nanorods and nanotubes

- Synthesis of these one-dimensional nanomaterials can be carried out by various techniques such as: (i) spontaneous growth (e.g., evaporation–condensation, vapor–liquid–solid growth, and stress-induced recrystallization), (ii) template-based synthesis (e.g., electroplating, electrophoretic deposition, colloid dispersion, melt or solution filling, and chemical reaction), (iii) electrospinning, and (iv) lithography.
- Spontaneous growth usually results in the formation of single-crystal nanowires or nanorods along a preferential direction of crystal growth. It depends on the crystal structures and the surface properties of the nanowire materials.
- For the formation of nanowires or nanorods, anisotropic growth is required, because the crystal needs to grow along a certain orientation faster than the other directions. The defects and impurities on the growth surfaces can cause non-

uniform products. Template-based synthesis usually produces polycrystalline or amorphous products. The details of these techniques have been presented by Cao (2006).

9.2.3.1 Nanowires and nanorods

- The nomenclature, *nanorod* and *nanowire*, is somewhat arbitrary. However, the terminology used in the literature suggests that they are distinguished by their diameter. The diameter of the nanorods is larger than nanowires, and the demarcation line is approximately 20 nm (Ozin and Arsenault, 2006).
- Pan *et al*. (2001) synthesized long ribbon-like nanostructures (known as *nanobelts*) of semiconducting oxides of zinc, tin, indium, cadmium and gallium by evaporating the commercial metal oxide powders at high temperatures (see Fig. 9.2.9).

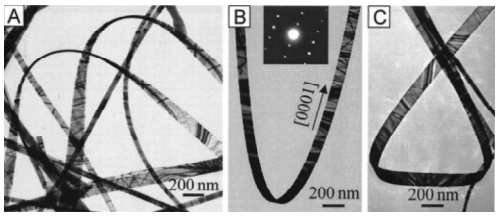

Fig. 9.2.9 TEM images of several straight and twisted ZnO nanobelts, displaying the shape characteristics of the belts (Pan *et al*., 2001) (reproduced by permission from The American Association for the Advancement of Science, © 2001).

- The oxide powder was placed at the center of an alumina tube and the tube was inserted in a horizontal tube furnace where the temperature, pressure and evaporation time were controlled. During evaporation, the products were deposited onto an alumina plate placed at the downstream end of the alumina tube.
- The deposited product was characterized and analyzed by X-ray diffraction, scanning electron microscopy, transmission electron microscopy and energy-dispersive X-ray spectroscopy. The oxide nanobelts were pure, structurally uniform and single crystalline. Most of them were free from defects and dislocations. They had rectangle-like cross-section with typical width between

30 and 300 nm, and length up to a few millimeters. The width-to-thickness ratio varied between 5 and 10.

- The belt-like morphology is a distinctive and common structural characteristic for the family of semiconducting oxides. By controlling the growth kinetics, left-handed helical nanostructures and nanorings may be formed by rolling up single crystal ZnO nanobelts. This phenomenon is attributed to a consequence of minimizing the total energy attributed by spontaneous polarization and elasticity.
- One of the most straightforward and general methods of synthesis of nanowires is by filling a template bearing nanosized cylindrical holes. For example, metal nanowires can be synthesized by the reduction of a metal salt into the cylindrical pores of a thin membrane. If a template containing very homogeneous pores is available, this technique can produce nanowires and nanorods having controlled size. There are many porous templates that fulfill such requirements. One important example is microporous zeolites, which can be filled with other materials. Chemically synthesized templates such as liquid-crystal-templated mesopourous aluminosilicates, electrochemically-synthesized templates such as anodically-etched aluminum or silicon, self-organized systems such as microphase-separated block copolymers, and track-etched polymer membranes can be used to make nanowires (Martin, 1994; Thurn-Albrecht *et al*., 2000) (see Fig. 9.2.10).
- Nanochannel silicon membranes with perfectly ordered pores have been prepared by various techniques. Such silicon membranes can be used to synthesize modulated-diameter gold nanorods (Ozin and Arsenault, 2006). This method has been adapted to create nanorods having different metal segments by electrodeposition. These modulated-composition nanorods are known as *nanobarcodes* due to their striped appearance. They may be utilized to tag molecules in analytical chemistry and biology.

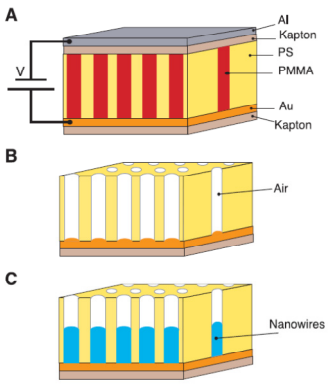

Fig. 9.2.10 A schematic representation of high-density nanowire fabrication in a polymer matrix. (A) An asymmetric diblock copolymer annealed above the glass transition temperature of the copolymer between two electrodes under an applied electric field, forming a hexagonal array of cylinders oriented normal to the film surface. (B) After removal of the minor component, a nanoporous film is formed. (C) By electrodeposition, nanowires can be grown in the porous template, forming an array of nanowires in a polymer matrix (Thurn-Albrecht *et al.*, 2000) (reproduced by permission from The American Association for the Advancement of Science, © 2000).

- Segment-specific anchoring of selected molecules to a barcode metal nanorod is known as *orthogonal self-assembly*. Suppose that the nanorod has two segments of different metals such as gold and platinum. An organic molecule that has same affinity for the two metals binds indiscriminately to the Au and Pt segments. However, an organic molecule that has greater affinity for Au displaces the former molecule from the segments constituted by Au. In this way, the two metals on the same nanorod can have two distinct monolayers of chemical species.
- The ability to anchor functional molecules to selective locations of a nanorod provides a number of interesting opportunities to direct the nanorods to self-assemble into predetermined functional architecture. An application of this method is DNA end-functionalization and detection of gold nanorods. Thiolated DNA is bound to the exposed ends of gold nanorods encased in an alumina membrane. The membrane is then dissolved in NaOH to create a suspension of gold nanorods end-functionalized with DNA. Rhodamine-

labelled complementary DNA is end-coupled to the nanorods. By a similar approach, DNA-side functionalized gold nanorods have been created and directed to self-assemble on soft-lithographically patterned gold surface sites, which had been functionalized with the complementary DNA.

- This technique of coverage of gold surfaces with gold nanowires by linking them with DNA offers good prospects for the assembly of wire structures with particular connectivity (see Fig. 9.2.11).

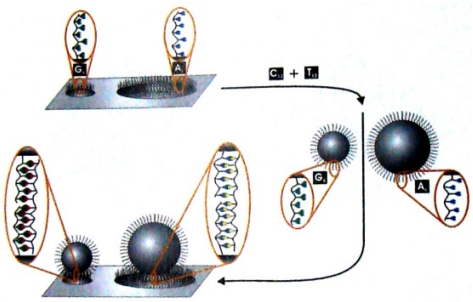

Fig. 9.2.11 A strategy for the orthogonal assembly of DNA-functionalized nanoparticle building blocks by dip-pen nanolithography (Ozin and Arsenault, 2006) (reproduced by permission from The Royal Society of Chemistry, © 2006).

- Nanowires have been organized by spinning them to form functional devices. The method is based on electrospinning. When a solution of a polymer such as polyvinylpyridine (or a polymer sol–gel mixture) passes through a high-voltage metal capillary, a thin charged stream emerges from the orifice. This continuous process generates a population of charged nanofibers that are driven to the ground electrode on a substrate.
- The dimensions of the electrospun nanowire depend on the solvent viscosity, conductivity, surface tension and the precursor concentration. The collector electrodes can be arranged in various configurations to coerce the nanowires into organized arrays. Using this procedure, single or multilayer architecture of nanowires can be created in a simple and reproducible manner.
- Hollow nanofibers of inorganic and inorganic–polymer hybrid materials have been prepared by electrospinning. The technique involves ejection from the double-capillary spinneret of a continuous coaxial jet comprised of a heavy

mineral oil core surrounded by a sheath of ethanol–acetic acid–PVP–Ti(O*i*Pr)$_4$. The composite core-shell nanofibers are collected on an aluminum or silicon substrate and allowed to hydrolyze at room temperature in air. Thereafter, the oily core is extracted with octane to leave behind a collection of nanotubes with the walls made of amorphous TiO_2 and PVP. Calcination in air at 773 K oxidizes the organic polymer and the amorphous titania is converted into the anatase polymorph.

- The template-based methods which use zeolites, membranes or nanotubes can control crystal growth but usually form nonuniform and polycrystalline materials. The vapor–liquid–solid (VLS) growth process is one of the most successful ways of synthesizing oriented single-crystal semiconductor nanowires with control over their diameter, length and composition.
- The original idea goes back to the 1960s when the vapor growth techniques were developed to produce crystalline semiconductors from hot gaseous reactants. It was discovered that whiskers of the semiconductor would spontaneously grow out of gold particles placed in the reaction chamber.
- In the VLS method of synthesis of nanowires, a catalyst first melts to form a droplet, becomes supersaturated with the precursors, and the precipitating elements extrude out of the catalyst droplet as a single-crystal nanowire. For example, silicon nanowire has been synthesized by laser-ablation of a Fe-Si target in a buffer gas, which creates a dense vapor that condenses into nanoclusters as the Fe and Si species cool through collisions with the buffer gas (see Fig. 9.2.12).
- The equilibrium pseudo-binary Fe–Si phase diagram is known. Therefore, the composition and temperature that favors liquid Fe–Si in equilibrium with solid Si can be identified. The furnace temperature is controlled to maintain Fe–Si in liquid state. The growth of Si nanowire begins only when the Fe–Si liquid nanocluster becomes supersaturated with Si. The growth of nanowire proceeds as long as the Fe–Si nanoclusters remain in the liquid state and Si-nutrient is available.

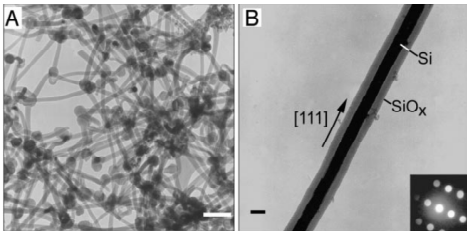

Fig. 9.2.12 (A) A TEM image of the nanowires produced after ablation of a $Si_{0.9}Fe_{0.1}$ target. Scale bar, 100 nm. (B) Diffraction contrast TEM image of a Si nanowire; crystalline material (the Si core) appears darker than amorphous material (SiO_x sheath) in this imaging mode. Scale bar, 10 nm. (Inset) Convergent beam electron diffraction pattern recorded along the [211] zone axis perpendicular to the nanowire growth axis (Morales and Lieber, 1998) (reproduced by permission from The American Association for the Advancement of Science, © 1998).

- The diameter of the nanowire is determined by the diameter of the nanoclusters and the length is controlled by the growth speed. The growth of nanowire terminates when it passes out of the hot zone of the reactor. A sheath of silica coats the surface of the wire and the catalytic Fe–Si nanocluster is attached to the end of the wire.
- Doping can be made by introducing controlled amounts of PH_3 (for n-Si nanowire) or BH_3 (for p-Si nanowire) in the gas phase during the growth process. Epitaxy at the interface between the nanocluster and nanowire is responsible for the oriented single-crystal growth. The VLS of SiH_4/H_2 gaseous mixture on gold nanocluster catalysts generates a narrow size distribution of single-crystal silicon nanowires having diameters as low as 3 nm.
- The growth of a nanowire occurs as follows. When the silicon species condenses at the surface of the droplet, the droplet becomes supersaturated with silicon. Subsequently, the supersaturated silicon diffuses from the liquid–vapor interface and precipitates at the solid–liquid interface resulting in the growth of silicon. The growth proceeds perpendicular to the solid–liquid interface. The rough liquid surface is composed of ledge, ledge-kink or kink sites. Every site over the entire surface can trap the impinging growth species. The catalyst not only acts as a sink for the growth species in the vapor phase, but it also aids in the deposition.

Consequently, the growth rate of the nanowires by the VLS method is very high in presence of the catalyst.

- The solubility depends on the surface energy and the radius of curvature of the surface which is given by the Kelvin equation (see Lecture 3 of Module 2). If facets are developed during the growth, the rates of lateral and longitudinal growths are determined by the growth of the individual facets. The nanowires have very small radius (i.e., large curvature). Therefore, for the growth of uniform nanowires and to prevent any significant growth on the side surface, the supersaturation should be kept low. If a high supersaturation is maintained, other facets would grow and secondary nucleation may occur on the growth surface, which can terminate the epitaxial growth.
- Using *in situ* microscopy in the germanium–gold system, Kodambaka *et al*. (2007) have shown that nanowire growth can occur below the eutectic temperature with either liquid or solid catalysts at the same temperature. They found that the state of catalyst depend on the growth pressure and the thermal history. They suggested that these phenomena may be due to the kinetic enrichment of the eutectic alloy composition.
- Chemical dopants (impurities that add or remove electrons) can be incorporated during the growth of the nanowires, and it is possible to ensure that the nanowire is n-doped (having extra conduction electrons) or p-doped (with some electrons removed to leave positively charged holes). Because a nanowire is elongated and easily polarized electrically, it is attracted towards a high electric field with which it lines up. Therefore, when a voltage is applied between two electrodes, a nearby nanowire suspended in liquid is drawn-in to bridge the gap between them. In this way, ordered rows of parallel single-nanowire bridges can be created. A junction can be created by placing a p-doped and an n-doped nanowire across each other (Duan *et al.*, 2001). A light-emitting diode can be created by this technique (see Lecture 1 of Module 1).

Exercise

Exercise 9.2.1: Answer the following questions clearly.

1. Explain the steps involved in the synthesis of nanoparticles using water-in-oil microemulsions.
2. What is percolation?
3. Explain how the Buckminsterfullerene was synthesized by Kroto *et al*. (1985). Explain the structure of the C_{60} molecule and its stability.
4. What are the large-scale synthesis methods of fullerenes?
5. Explain why fullerenes with $n = 24$, 28, 32, 36, 50, 60 and 70 are more stable as compared to their neighbors.
6. Explain the difference between a nanowire and a nanorod.
7. Mention three methods for the synthesis of nanowires and nanorods.
8. What is orthogonal self-assembly? What is its significance?
9. Explain how nanowires can be synthesized by the VLS method.
10. What is the role of catalyst in the VLS method?

Suggested reading

Textbook

- P. Ghosh, *Colloid and Interface Science*, PHI Learning, New Delhi, 2009, Chapter 11.

Reference books

- G. A. Ozin and A. C. Arsenault, *Nanochemistry*, RSC Publishing, Cambridge, 2006, Chapters 1–6.
- G. Cao, *Nanostructures and Nanomaterials*, Imperial College Press, London, 2006, Chapters 1–6.

Journal articles

- A. M. Morales and C. M. Lieber, *Science*, **279**, 208 (1998).
- C. R. Martin, *Science*, **266**, 1961 (1994).
- E. Matijević, *J. Colloid Interface Sci*., **58**, 374 (1977).
- H. -F. Eicke, *J. Colloid Interface Sci*., **56**, 168 (1976).
- H. W. Kroto, J. R. Heath, S. C. O'Brien, R. F. Curl, and R. E. Smalley, *Nature*, **318**, 162 (1985).
- H. W. Kroto, *Nature*, **329**, 529 (1987).
- I. Capek, *Adv. Colloid Interface Sci*., **110**, 49 (2004).
- P. Barnickel, A. Wokaun, W. Sager, and H. F. Eicke, *J. Colloid Interface Sci*., **148**, 80 (1992).
- S. Kodambaka, J. Tersoff, M. C. Reuter, and F. M. Ross, *Science*, **316**, 729 (2007).
- S. Zhou, C. Burger, B. Chu, M. Sawamura, N. Nagahama, M. Toganoh, U. E. Hackler, H. Isobe, and E. Nakamura, *Science*, **291**, 1944 (2001).
- T. S. Ahmadi, Z. L. Wang, T. C. Green, A. Henglein, and M. A. El-Sayed, *Science*, **272**, 1924 (1996).

- T. Thurn-Albrecht, J. Schotter, G. A. Kästle, N. Emley, T. Shibauchi, L. Krusin-Elbaum, K. Guarini, C. T. Black, M. T. Tuominen, and T. P. Russell, *Science*, **290**, 2126 (2000).
- W. Krätschmer, L. D. Lamb, K. Fostiropoulos, and D. R. Huffman, *Nature*, **347**, 354 (1990).
- X. F. Duan, Y. Huang, Y. Cui, J. F. Wang, and C. M. Lieber, *Nature*, **409**, 66 (2001).
- Y. Xie, Y. Qian, W. Wang, S. Zhang, and Y. Zhang, *Science*, **272**, 1926 (1996).
- Z. W. Pan, Z. R. Dai, and Z. L. Wang, *Science*, **291**, 1947 (2001).